ANS RPSD 2014 - 18th Topical Meeting of the Radiation Protection & Shielding Division of ANS
Knoxville, TN, September 14 – 18, 2014, on CD-ROM, American Nuclear Society, LaGrange Park, IL (2014)

SAND2014-2494C

ITS version 6.4: The Integrated TIGER Series of Monte Carlo Electron/Photon Radiation Transport Codes

Thomas. W. Laub, Ronald. P. Kensek, Brian C. Franke, Martin J. Crawford, Greg D. Valdez

Sandia National Laboratories, P.O. Box 5800, Mail Stop 1179, Albuquerque, NM 87185-1179
rpkense@sandia.gov, twlaub@sandia.gov, bcfrank@sandia.gov, mjcrawf@sandia.gov, gdvalde@sandia.gov

INTRODUCTION

ITS[1] (Integrated TIGER Series) is a suite of fully coupled electron/photon Monte Carlo radiation transport codes. The package contains programs to perform 1D, 2D and 3D simulations. The 3D geometry representations include the traditional combinatorial geometry (CG), facet-based models, CAD models for those users who have a license for the ACIS® CAD libraries, and hybrid models of any combination. There is a multigroup version which permits adjoint analysis. The availability of source code permits the more sophisticated user to tailor the code to specific applications and to extend the capabilities of the codes to more complex applications. ITS is presently available only through a U.S.-government-use license. It is available once again through the Radiation Safety Information Computational Center (RSICC).

NEW GEOMETRY CAPABILITIES

CAD-Based Geometry

Monte Carlo radiation transport codes traditionally utilize a native geometry description based on some form of CG. ITS version 6.4 has added the capability to use CAD-based geometry in the ACIS® format. CAD geometry query capability is implemented through ACIS® CAD libraries, which can be licensed separately through Spatial Corporation (http://www.spatial.com).

The ability to track directly on CAD geometry can shorten the laborious setup time enormously for a high-fidelity model. A drawback of tracking on CAD geometry is that the speed of particle tracking suffers. This is probably because the CAD geometry interrogation routines are not optimized for non-CAD related computations. However, trading analyst time for computer time is sometimes more economical. Figure 1 indicates the level of detail that can be contained in a single CAD part. Full CAD geometries can contain thousands of parts. Of course the ability to track particles on CAD geometries is also integrated into the parallel computational abilities of ITS. A recent production application demonstrated great parallel efficiency while using up to 64,000 processors on Los Alamos National Laboratory's "cielo" platform.

Fig. 1. Example of a complicated CAD geometry part.

Facet-Based Geometry

ITS has also implemented facet-based geometry tracking. The facet-based geometry capability was initially envisioned as a way to replace Non-uniform Rational B-spline (NURB) surfaces in CAD geometries. Spline surfaces are particularly compute-intensive when encountered during particle tracking. If a spline surface figures prominently in a calculation the slow down with respect to CAD geometry without spline surfaces can be as high as a factor of 1000. Replacing a CAD body containing a spline surface with a facetted body can significantly increase a calculation's efficiency.

An entire geometry can consist of facetted entities. The format of the facet-based geometry file is currently that exported by CUBIT.[2] CUBIT is a Sandia geometry and mesh-creation toolkit that is available to the public through a third party. The facet-based geometry tracking is native to ITS and does not require a license for third party libraries. Figure 2 shows one application of facet-based geometry. The geometry was created from the Visible Human Project® to demonstrate a simulated x-ray on a model using over a million facets. The detector was a simple rectangular parallelepiped in our combinatorial geometry.

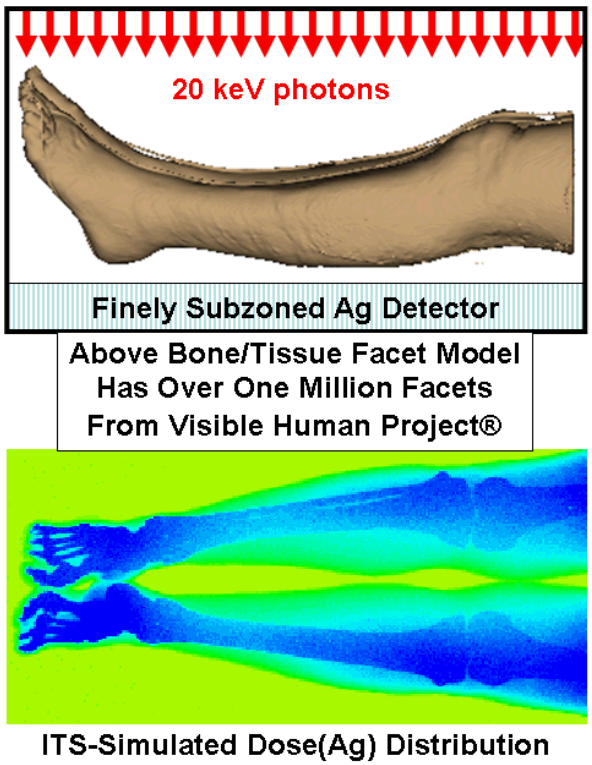

Fig. 2. Example calculation using facet-based geometry.

Hybrid Geometry

The facet-based geometry example mentioned above also demonstrates the hybrid geometry capability. Any of the three geometry types available in ITS can be used together. Individual parts of the geometry can be CG, CAD, or facetted. In fact, individual surfaces of CAD parts can be replaced with a facetted surface. In the simulated x-ray example the detector was a CG simple rectangular parallelepiped. The resolution of the simulated x-ray was controlled using the ITS automatic subzoning feature.

NEW OUTPUT CAPABILITIES

Automatic Subzoning

Another feature of ITS is automatic subzoning. The feature allows users to easily create spatially-differential tallies. There are dozens of shapes and subzoning structures which may be overlaid on our geometry representations. The user does not have to actually cut up larger geometry sections to obtain a spatially-varying dose distribution. Subzoning is tied to zones and does not overlay arbitrary volumes of the geometry. The automatic subzoning structures can exactly match a CG zone or can be overlaid on non-regular geometry zones. Figure 3 illustrates just a couple of the automatic subzoning structures available. The first is an RCC-TRC that is a right-circular cylinder for the outer boundary and a truncated right cone for the inner boundary. The second is a toroidal shell where both outer and inner boundaries are tori.

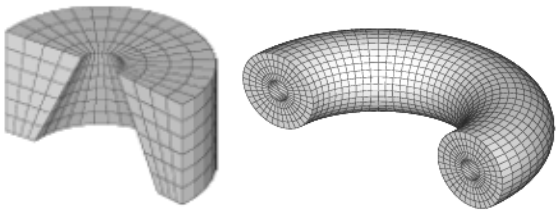

Fig. 3. Two examples of automatic subzoning structures.

Finite Element-Like Output

A side benefit of the automatic subzoning is that a subzoned tally (currently only energy and charge deposition) can be written to a finite element formatted file. Currently the output is in Tecplot®[3] format but there is also a tool to convert the file to the popular Exodus[4] format. The finite element format can be used to transfer results to downstream applications like mechanical simulation codes. In addition, the finite element format can be used with a plethora of visualization tools. However, visualization can be low resolution if the subzoning scheme was an overlay that did not conform to the boundaries of the zone.

MULTIGROUP AND ADJOINT CAPABILITY

The ITS suite of codes includes a multigroup version (along with the multigroup cross section generator CEPXS).[5] The main advantage of the multigroup version is the ability to perform adjoint calculations. To first order, this suggests running the problem "backwards." In a forward run, the specification of a single source leads to many detector responses (dose distributions, charge distributions, escaping particles, etc). In an adjoint calculation, a single detector response (e.g., dose at a single point or volume) leads to the result of that detector response for various sources (incoming directions, spectra). So the user can determine a detector response once and fold that response with many different spectra instead of running a forward calculation for each source spectrum of interest.

We mostly use the adjoint capability in 3D mode to assess the response from all directions over the sphere of 4π incoming directions. The incoming phase space is discretized into what we call the "direction sphere" by specifying the number of polar angular bins desired. The sphere is then divided up into roughly equal-solid-angle "pixels." As adjunctons (adjoint particles) move from the detector point or volume out of the geometry the tally is scored in the angular pixel through which the particle

exited. After folding the direction sphere of response functions with any desired source spectrum, a visualization of the direction sphere gives the analyst an idea of what direction may allow more particles to reach the detector. Figure 4 is an example of dose in the center of the illustrated geometry resulting from a photon spectrum coming from many directions. The visualization is produced using Tecplot® but the output file is formatted as 2D finite elements so other finite-element visualization tools can also be used. There is also a ray-tracing capability associated with the direction sphere that allows very fine resolution scoping calculations to look for geometric details that might be important.

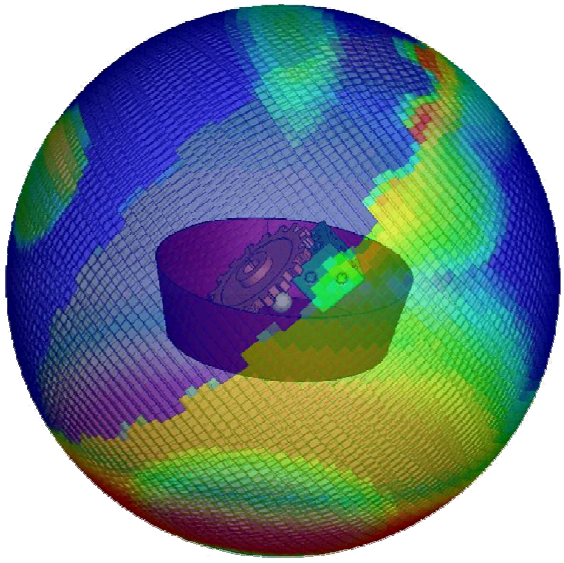

Fig. 4. Adjoint direction sphere visualization of dose.

COMING FEATURES

Time Binning

The next release of ITS will contain time-binned sources and tallies. The capability has been initially implemented and testing is in progress. Tracking particle age (time) is trivial for photons since they all travel at the same speed all of the time—the speed of light. However, tracking the age of other particles whose speed varies with their energy is a bit more complex. ITS uses the condensed history method along with the continuous slowing down approximation for the electron transport model. In the condensed history method the effect of the many small-change interactions that electrons go through are accumulated and applied after the fact at the end of an electron substep. Multiple-scattering theory is used to generate the distributions used in condensed history methods. The continuous slowing down approximation (CDSA) assumes that the energy of an electron decreases linearly between "collisions" but ITS goes beyond simple CDSA and includes other energy loss effects.

In our implementation of electron travel time we started with a formulation developed by Halbleib[6]. The passage of time t for an electron with speed ν traveling a distance s is:

$$t = \frac{s}{\beta c}, \text{ where } \beta = \nu/c.$$

However, the electron's speed changes over the course of the step as its energy changes, so we have an integral:

$$t = \int \frac{ds}{\beta c}.$$

Changing to an energy variable for integration over the distance:

$$t = \int \frac{dE}{\beta c \frac{dE}{ds}}.$$

Instead of simply using the total stopping power dE/ds, we use the sampled energy loss (which includes energy straggling and loss due to sampled bremsstrahlung photons) ΔE over the distance s.

$$\Delta t = \frac{\Delta E}{\beta c \frac{\Delta E}{\Delta s}}$$

After some manipulation, variable definitions, and substituting $E_1 = E_0 - \Delta t$ the equation for Δt is finally implemented as:

$$\Delta t = \frac{\Delta E}{\beta c \frac{\Delta E}{\Delta s} - \frac{E_0}{\gamma}},$$

where γ is the total electron energy, including rest mass energy, divided by the rest mass energy.

Low-Energy Transport

Currently below-1-keV transport for photons (absorption only) has been implemented in the development version of ITS. We are working on implementing full transport capability for both photons and electrons using the Livermore data implementation.[7,8,9]

Alternate Electron Transport Algorithms

We are working on implementing alternate electron transport algorithms. One alternate form is called Generalized Boltzmann Fokker-Planck (GBFP).[10] The method rigorously preserves cross section moments in the solution of a Boltzmann transport equation. GBFP shows promise in simplifying material boundary-crossing issues in electron transport.

Another alternate algorithm is analog electron transport and is being implemented in conjunction with low-energy electron cross sections.

Stochastic Media Transport

Stochastic media problems arise when the mean chord lengths through materials are larger than the transport mean free path, such that material homogenization cannot be used, but small enough that geometry realizations cannot be efficiently analyzed. Stochastic-media simulations require numerous boundary crossings. The ITS team is investigating using the Levermore-Pomraning (LP) closure[11] to improve ITS handling of stochastic media.[12]

AVAILABILITY

ITS is available through the Radiation Safety Information Computational Center[13] (RSICC) as code package C00792. Unfortunately, it is currently only available under a government-use-only license. We hope to be able to expand the availability. The distribution includes source code, a build system, a testing system, documentation, and some tools for output manipulation. Without any further licenses the CG and facet-based geometry representations are included. You do need CUBIT or some other tool to generate the facetted representation from a CAD model.

ACKNOWLEGEMENTS

Sandia is a multi-program laboratory managed and operated by Sandia Corporation, a wholly owned subsidiary of Lockheed Martin Company, for the United States Department of Energy's National Nuclear Security Administration under contract DE-AC04-94AL85000.

REFERENCES

1. Franke, Brian, et al., "ITS Version 6: The Integrated TIGER Series of Coupled Electron/Photon Monte Carlo Transport Codes, Revision 5," SAND2008-3331, Sandia National Laboratories, PO Box 5800, Albuquerque, NM. 87185, September 2013.
2. CUBIT Geometry and Mesh Generation Toolkit, Sandia National Laboratories, PO Box 5800, Albuquerque, NM. 87185, https://cubit.sandia.gov.
3. Tecplot 360 User's Manual, Release 1, Tecplot Inc, Post Office Box 52708, Bellevue, WA 98015-2708, www.tecplot.com.
4. Schoof, Larry, et al., "Exodus II: A Finite Element Data Model," SAND92-2137, Sandia National Laboratories, PO Box 5800, Albuquerque, NM. 87185, November 1995.
5. Morel, et al., "A Hybrid Multigroup/Continuous-Energy Monte Carlo Method for Solving the Boltzmann-Fokker-Planck Equation," NSE, 124, 369-389 (1996).
6. Halblieb, John A., "Time-Dependent Monte Carlo Deposition Rate From Flash X-Ray Sources," IEEE Transactions on Nuclear Science, Vol. NS-29, No. 6, December 1982.
7. S.T.Perkins, D.E.Cullen, S.M.Seltzer, "Tables and Graphs of Electron-Interaction Cross Sections from 10 eV to 100 GeV Derived from the LLNL Evaluated Electron Data Library (EEDL), Z=1,100", UCRL-50400 Vol 31, (1991).
8. D.E.Cullen, M.H.Chen, J.H.Hubbell, S.T.Perkins, E.F.Plechaty, J.A.Rathkopf, and J.H.Scofield, "Tables and Graphs of Photon-Interaction Cross Sections from 10 eV to 100 GeV Derived from the LLNL Evaluated Photon Data Library (EPDL)", UCRL-50400 Vol 6, (1989).
9. S.T.Perkins, D.E.Cullen, M.H.Chen, J.H.Hubbell, J.Rathkopf, J.Scofield, "Tables and Graphs of Atomic Subshell and Relaxation Data Derived from the LLNL Evaluated Atomic Data Library (EADL), Z=1,100", UCRL-50400 Vol 30, (1991).
10. B.C. Franke, A.K. Prinja, L.T. Harding, "Monte Carlo Electron Transport Using Generalized Boltzmann Fokker-Planck Scattering Models", Mathematics and Computation, Supercomputing, Reactor Physics and Nuclear and Biological Applications, Palais des Papes, Avignon, France, September 12-15, 2005.
11. M. Adams, E. Larsen, and G. Pomraning, "Benchmark Results for Particle Transport in a Binary Markov Statistical Medium," J. Quant. Spectrosc. Radiat. Transfer, 42, 253-266 (1989).
12. B.C. Franke, R.P. Kensek, A.K. Prinja, "Evaluation of Monte Carlo Electron-Transport Algorithms in the Integrated Tiger Series Codes for Stochastic-Media Simulations," Joint Intl. Conf. on Supercomputing in Nucl. Appl. and Monte Carlo 2013 (SNA + MC 2013), La Cité des Sciences et de l'Industrie, Paris, France, October 27-31, 2013.
13. RSICC, Radiation Safety Information Computational Center, Oak Ridge National Laboratory, P.O. Box 2008 Oak Ridge, TN 37831, https://rsicc.ornl.gov/Default.aspx, https://rsicc.ornl.gov/PackageDetail.aspx?p=ITS6&id=C00792&cpu=PCX86&v=00&t=Integrated%20TIGER%20Series%20of%20Coupled%20Electron/Photon%20Monte%20Carlo%20Transport%20Codes%20System.